

FERA: A Pose-Based Semantic Pipeline for Automated Foil Fencing Refereeing

Ziwen Chen

Marc Garneau Collegiate Institute (TDSB)
Toronto, Canada

ziwen08@gmail.com

Zhong Wang

Beijing Institute of Mathematical Sciences and Applications (BIMSA)
Beijing, China

wangzhong@bimsa.cn

Abstract

Many multimedia tasks map raw video into structured semantic representations for downstream decision-making. Sports officiating is a representative case, where fast, subtle interactions must be judged via symbolic rules. We present FERA (**F**encing **R**eferee **A**ssistant), a pose-based framework that turns broadcast foil fencing video into action tokens and rule-grounded explanations. From monocular footage, FERA extracts 2D poses, converts them into a 101-dimensional kinematic representation, and applies an encoder-only transformer (FERA-MDT) to recognize per-fencer footwork, blade actions, and blade-line position. To obtain a consistent single-fencer representation for both athletes, FERA processes each clip and a horizontally flipped copy, yielding time-aligned left/right predictions without requiring a multi-person pose pipeline. A dynamic temporal windowing scheme enables inference on untrimmed pose tracks. These structured predictions serve as tokens for a language model (FERA-LM) that applies simplified right-of-way rules to generate textual decisions. On 1,734 clips (2,386 annotated actions), FERA-MDT achieves a macro-F1 of 0.549 ± 0.018 under 5-fold cross-validation, outperforming BiLSTM and TCN baselines. Combined with FERA-LM, the full pipeline recovers referee priority with 77.7% accuracy on 969 exchanges. FERA provides a case-study benchmark for pose-based semantic grounding in a two-person sport and illustrates a general pipeline for connecting video understanding with rule-based reasoning.

Keywords. Human pose estimation, action recognition, multi-label classification, sports officiating

1. Introduction

Understanding human activities from video is a central problem in multimedia analysis. Many decision-making tasks require not only recognizing actions, but also converting them into structured representations that support higher-level reasoning or explanation. Sports officiating is a compelling example: actions unfold rapidly, interactions are fine-grained, and final judgments depend on applying symbolic rules to visual evidence.

Foil fencing is a challenging instance of this broader problem. Referees must track two fencers, interpret fast blade exchanges, and apply right-of-way (priority) rules to decide who is awarded the point when hits occur in close succession. Even at elite competitions, calls can be controversial; in practice settings, trained officials may not be available. While electronic scoring indicates *when* a touch occurs, it does not explain *why* a point is awarded. Automating such judgments requires bridging the semantic gap between raw video and rule-based reasoning.

Recent work has begun to close this gap in other sports, for example through multi-view video assistant referee systems and event spotting benchmarks for soccer [6, 9, 10], as well as pose-conditioned temporal models for skeleton-based action recognition [2, 26]. These highlight sports officiating as an emerging AI application with a path toward deployment. We empirically study whether 2D skeletons with engineered kinematic features are sufficient for this task in broadcast fencing video, and how feature design, dynamic windows, and calibration affect recognition quality.

We treat fencing exchanges as a constrained but representative setting in which video must be translated into tokens suitable for symbolic reasoning. Our goal is to predict, from monocular video, (i) the multi-label set of footwork and blade actions active for each fencer over time

and (ii) the instantaneous blade-line position. To simplify all downstream processing and avoid fencer-specific logic, we extract per-fencer sequences by applying the same single-fencer pipeline to the original clip and to a horizontally flipped copy. This yields two time-aligned left-facing views—one for each athlete—while keeping detection, tracking, and feature extraction identical for both sides.

Our framework, FERA, separates perception from reasoning. First, 2D poses are converted into a 101-dimensional kinematic feature sequence in a canonical single-fencer view. Second, an encoder-only transformer (FERA-MDT) is trained on trimmed exchanges and deployed on arbitrary-length pose tracks using dynamic temporal windows to infer segment boundaries. Finally, paired left/right predictions are converted into tokens and fed to a language model (FERA-LM) that applies a simplified subset of foil rules to generate textual decisions and concise explanations.

Contributions.

- We introduce a pose-based pipeline (FERA) that maps broadcast foil footage into multi-label action and blade-line tokens and then into rule-grounded explanations for referee assistance in two-person weapon sports, achieving 77.7% agreement with referee priority on 969 exchanges.
- We propose a kinematic feature representation and calibrated transformer backbone (FERA-MDT) for multi-label move and blade recognition with dynamic temporal windowing, combining pose estimation with scale-robust geometric and motion features.
- We provide a case-study dataset with frame-level annotations of 12 moves and 5 blade-line positions from broadcast foil video, providing (to our knowledge) the first benchmark for pose-based multi-label move and blade recognition in foil, together with code and baselines for pose-level semantic grounding.

2. Related Work

2.1. AI for sports refereeing

Several works have explored AI-assisted refereeing and decision support in sports. In fencing, prior work has focused mainly on controlled footwork datasets: FenceNet and related models report high accuracy on the Fencing Footwork Dataset [17, 28], which contains 652 videos from 10 fencers recorded under fixed camera angles and annotated with a small set of footwork actions. While valuable for isolated motion analysis, these datasets omit blade actions, opponent interactions, and real broadcast conditions, limiting their applicability to foil referee decisions.

In soccer, Video Assistant Referee Systems (VARs) combine multi-view analysis with temporal localization of

fouls and offside events [9, 10], and benchmarks such as SoccerNet target decision-making and explanation quality in realistic broadcast footage [6]. Unlike SoccerNet-style event spotting, which focuses on second-level events in multi-view soccer, our task operates on single-view broadcast footage and requires frame-level multi-label recognition and rule reasoning in a two-person weapon sport. FERA extends this line of work to foil fencing, where exchanges are short, motion is fast and mostly linear, contacts are point-based, and right-of-way depends on subtle blade actions and timing.

2.2. Pose-based action recognition

Human pose estimation supports action recognition by mapping video to joint trajectories. Bottom-up multi-person methods such as OpenPose [4] introduced part affinity fields, while top-down approaches combine person detection with single-person pose estimators [25]. Transformer-based models like ViTPose [26] further improve accuracy via large-scale pretraining. We adopt a standard detection–pose stack, using MMDetection and MMPose [5, 18] with RTMDet and RTMPose [12, 16] for efficient fencer detection and 2D keypoint estimation.

For temporal modeling, recurrent networks, temporal convolutional networks (TCN) [2], and transformers have all been explored for skeleton-based action recognition, with growing interest in calibrated probabilities [8]. Existing pose-based datasets, however, focus on everyday actions or sports without handheld weapons and therefore ignore fine-grained bilateral interactions. In fencing, foil blades move quickly and are often blurred or absent in low-frame-rate broadcast footage, making explicit geometric blade reconstruction unreliable.

This setting motivates models that infer blade-line implicitly from body dynamics (e.g., wrist–elbow configuration, arm extension, timing) rather than from direct blade detection. Our method follows this strategy by jointly learning moves and blade-line from pose-derived kinematic features.

3. Dataset

3.1. Source videos and clip extraction

The FERA dataset is constructed from professional foil bouts recorded at three Grand Prix competitions (720p, 25 fps), covering approximately 130 competitors. For each match, we locate candidate exchange segments by scanning for changes in the electronic scoreboard and hit lights. Static overlays for score and hit indicators are localized once per event, and color and digit recognition are used to detect hits and score changes. These signals are used only to align clips with official referee decisions.

Each match is segmented into short clips containing the



Figure 1. Custom labeler for per-fencer moves and blade positions. Visualized pose estimates help identify labeling or tracking failures; clips with unreliable fencer selection are discarded.

final seconds preceding a touch. We retain clips with clear views of the piste and both fencers, and discard segments where camera cuts or occlusions prevent reliable tracking.

All source videos are publicly available competition recordings; we release only anonymized pose features, labels, and code.

3.2. Annotation protocol

Each clip has a unique identifier and is converted to a canonical left-facing view: in the original clip the annotator labels the left fencer; in a horizontally flipped copy, the original right fencer (now on the left) is labeled. All annotations were produced by the first author (a competitive foil fencer with nine years of experience) using slowed replay and frame-by-frame scrubbing.

Using a custom tool (Fig. 1), the annotator labels continuous time intervals with one or more actions from the 12-class vocabulary in Table 1(a) and a single blade-line position in {4, 6, 7, 8, other}. In the standard foil convention, position 4 denotes high inside line, 6 high outside, 7 low inside, and 8 low outside. Overlapping actions (e.g., beat plus step forward) receive all relevant labels. Intervals are expanded to frame-level multi-hot vectors, and ambiguous exchanges are revisited for consistency. When both sides are annotated, a clip yields two single-fencer sequences with the same identifier; FERA-MDT is trained only on these canonical single-fencer sequences.

3.3. Data distribution

We work with 1,734 clips and 2,386 annotated actions across all single-fencer sequences. On average, each example contains 1.38 moves. Table 1 summarizes the distributions of move labels and blade positions.

All experiments use 5-fold multilabel-stratified cross-validation at the clip level, ensuring that no frames from a clip appear in both training and test sets. We do not enforce disjoint fencers across folds because athlete identity is not consistently available in broadcast metadata.

Table 1. Distributions of moves and blade positions.

(a) Moves			(b) Blade positions		
Move	Count	%	Position	Count	%
Step forward	687	28.8	6	1114	64.2
Step backward	349	14.6	8	410	23.6
Half step forward	127	5.3	7	95	5.5
Half step backward	87	3.6	4	85	4.9
Lunge	232	9.7	Other	30	1.7
Flèche	11	0.5			
Wait	71	3.0			
Parry	72	3.0			
Beat	150	6.3			
Counterattack	77	3.2			
Fake	49	2.1			
Hit	474	19.9			

3.4. Data augmentation

After splitting into folds, we apply data augmentation to improve robustness. Augmentations include temporal jitter, additive noise, small rotations, and scaling. Minority moves are oversampled, and blade-line imbalance is addressed via loss weighting. At evaluation time, per-class thresholds and temperature scaling tuned on validation sets yield calibrated probabilities.

4. Method

The FERA framework follows a modular perception-to-reasoning pipeline (Fig. 2). Starting from monocular broadcast video, the system first detects and tracks individual fencers, extracts 2D human poses, and converts them into a canonical single-fencer representation. These pose sequences are mapped to kinematic feature tokens and processed by a temporal model (FERA-MDT) to recognize multi-label actions and blade-line positions over time. Finally, the structured predictions from both fencers are aggregated into symbolic tokens and passed to a language-based reasoning module (FERA-LM), which applies simplified right-of-way rules to generate a referee decision and explanation.

4.1. Pose tracking

We obtain per-fencer pose tracks using a top-down detect–pose–track pipeline (detect persons, estimate single-person pose, then associate tracks over time). RTMDet-Tiny (MMDetection) detects person bounding boxes and RTMPose-M (MMPose) extracts 2D joints for each detected person [5, 12, 16, 18]. Detections are linked over time using Norfair [21, 22] with a distance combining box IoU and centroid distance. If an ID is lost, it is recovered by matching new detections to the most recent boxes. Joint trajectories are smoothed with an exponential moving average to reduce short-term jitter while preserving fast fencing motion.

We then select the target fencer track in each view with

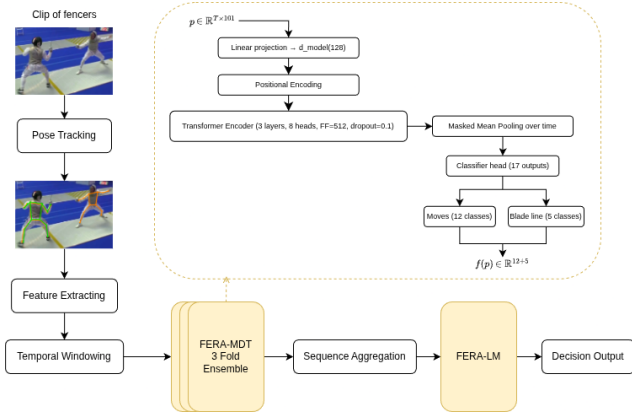


Figure 2. FERA multimedia pipeline from broadcast foil video to referee decision. Yellow denotes the FERA components.

lightweight filtering and scoring. In the first few frames, we suppress obvious non-target detections by retaining only boxes whose vertical centers fall within a central action band and whose areas exceed a minimum fraction of the frame, removing small background detections and spectators near the image borders. During tracking, we apply a looser area filter and rely on temporal continuity.

To further reject non-fencers (e.g., referees), we apply a fencer-candidate test based on detector confidence, box size, and pose geometry. Very small or low-score tracks are dropped; when poses are available, each track is associated with its most-overlapping pose and candidates with joints concentrated near the bottom of the frame are discarded, which commonly corresponds to referees off the piste. Among remaining tracks, a foreground score favors large, upright people on the left side and penalizes boxes near the top/bottom borders; scores are accumulated over the first 15 frames and the best track is selected.

This procedure is run on the original clip and on a horizontally flipped copy, yielding two canonical left-facing single-fencer tracks (one per athlete) that share the same frame indices and are naturally time-aligned. Finally, tracks are mapped to a canonical left-facing coordinate system to ensure geometric consistency with the annotation convention in Section 3.2.

4.2. Feature extracting

After removing head keypoints, each frame is represented by 12 body joints (shoulders, elbows, wrists, hips, knees, ankles) in the canonical left-facing coordinate system. Upstream processing normalizes these keypoints for translation and approximate scale, and missing or unreliable joints are set to zero.

From these normalized joints and precomputed joint angles, we build a 49-dimensional static descriptor per frame:

- **Normalized joints (24D)**: flattened (x, y) coordinates for

the 12 joints.

- **Center of mass (2D)**: mean of all nonzero joint coordinates.
- **Pairwise distances (11D)**: distances for a fixed set of segments and widths (upper/lower arm and leg segments, shoulder and hip width, and hand separation).
- **Joint angles (4D)**: left/right elbow and left/right knee angles.
- **Torso orientation (2D)**: sine and cosine of the angle of the shoulder-hip axis.
- **Arm extension (6D)**: for each arm, the shoulder-wrist distance and the corresponding unit direction vector (2D).

To capture motion, we append first- and second-order finite differences for (i) the 24 normalized joint coordinates and (ii) the 2D center of mass, contributing 52 additional dimensions. The final per-frame descriptor therefore has 49 static + 52 motion = 101 features and is used as the input token representation for FERA-MDT.

4.3. Temporal windowing

FERA-MDT is trained on trimmed single-fencer segments in which all active moves share the same temporal boundary: if a beat occurs during a step forward, both labels are attached to the same frame interval. At inference time, the model therefore predicts, for each input sequence, a multi-label set of moves that are assumed to share a single start and end frame, together with one blade-line class.

In deployment, FERA-MDT must operate on per-fencer pose tracks of arbitrary length, where segment boundaries are unknown. We use a dynamic temporal windowing strategy to discover these boundaries. Given a tracked pose sequence for one fencer (25 fps), we start from frame s with a short window and gradually expand it up to a maximum of 60 frames (about 2.4 s). For each candidate window we evaluate a 3-model FERA-MDT ensemble, where each model is trained on a different training fold and produces 12 move probabilities and a 5-way blade distribution. This windowing-and-ensemble procedure is used only for deployment on untrimmed tracks; cross-validation metrics in Section 5 use one model per fold on trimmed segments.

For a move class c to be accepted in the current window, at least two out of three models must predict $p_c > \tau_c$, where τ_c is the per-class threshold tuned on validation data. The blade-line class for the window is chosen by majority vote over the three models' blade predictions. If at least one move class is accepted, we record the current window $[s, e]$ as a segment with a multi-label move set and a single blade-line label and resume from frame $e+1$. If no move is accepted by the maximum window length, we slide the start frame forward by one and repeat. This yields an ordered sequence of non-overlapping segments; co-occurring moves (e.g., step forward + beat) share the same temporal window and thus the same boundaries.

Processing each bout twice (original and horizontally flipped) yields two canonical single-fencer views that share the same global frame indices. As a result, downstream comparison and right-of-way reasoning require no explicit multi-person pose association, identity tracking, or cross-person synchronization.

4.4. FERA-MDT

FERA-MDT is an encoder-only transformer for multi-label move and blade recognition. Given a sequence of T frames with 101-dimensional features $x_t \in \mathbb{R}^{101}$, each frame is projected to a 128-dimensional embedding

$$z_t = W_{\text{in}}x_t + b_{\text{in}} + p_t, \quad (1)$$

where $W_{\text{in}} \in \mathbb{R}^{128 \times 101}$, $b_{\text{in}} \in \mathbb{R}^{128}$, and $p_t \in \mathbb{R}^{128}$ is a learned positional embedding. Three transformer encoder layers (8 heads, FFN dimension 512, dropout 0.2) process the sequence. Valid frames are indicated by a mask $m_t \in \{0, 1\}$, and the sequence-level representation $h \in \mathbb{R}^{128}$ is computed by a masked mean

$$h = \frac{1}{\sum_t m_t} \sum_{t=1}^T m_t \hat{z}_t, \quad (2)$$

where $\hat{z}_t \in \mathbb{R}^{128}$ denotes the encoder output at time t .

A linear classifier outputs logits for the 12 move labels ($\ell_c^{(\text{move})}$) and 5 blade-line classes ($\ell_k^{(\text{blade})}$):

$$\ell = W_{\text{cls}}h + b_{\text{cls}}. \quad (3)$$

Move logits use a weighted binary cross-entropy loss

$$\mathcal{L}_{\text{move}} = - \sum_{c=1}^{12} w_c \left[y_c \log \sigma(\ell_c) + (1 - y_c) \log (1 - \sigma(\ell_c)) \right], \quad (4)$$

where $\ell_c \equiv \ell_c^{(\text{move})}$ denotes the move logit for class c , $y_c \in \{0, 1\}$ indicates the presence of move c , and $\sigma(\cdot)$ denotes the logistic sigmoid. Here, w_c are class weights to counter move imbalance.

Blade-line prediction uses a class-weighted cross-entropy

$$\mathcal{L}_{\text{blade}} = - \sum_{k=1}^5 \alpha_k \mathbf{1}[k = y^{\text{blade}}] \log \frac{e^{\ell_k^{(\text{blade})}}}{\sum_j e^{\ell_j^{(\text{blade})}}}, \quad (5)$$

where $y^{\text{blade}} \in \{1, \dots, 5\}$ is the blade-line label and $\mathbf{1}[\cdot]$ is the indicator function. The total loss is

$$\mathcal{L} = \mathcal{L}_{\text{move}} + \lambda_{\text{blade}} \mathcal{L}_{\text{blade}}, \quad (6)$$

with $\lambda_{\text{blade}} = 0.677$ chosen to balance gradient magnitudes. Training uses AdamW [15] (10^{-3} learning rate, 10^{-4} weight decay) with warmup, flat, and cosine-decay phases.

4.5. Sequence aggregation

FERA-MDT produces two ordered lists of single-fencer segments,

$$S_i^{(L)} = (s_i, e_i, M_i^{(L)}, B_i^{(L)}), \quad S_j^{(R)} = (s_j, e_j, M_j^{(R)}, B_j^{(R)}),$$

where $[s, e]$ denotes the frame range, M the multi-label move set, and B the blade-line class. Because the flipped clip is a horizontal mirror of the original, both lists share the same global frame indices and are naturally time-aligned.

For each fencer, segments are serialized into a compact representation containing start/end frames, move identifiers and names, and blade-line names, and formatted into a textual script in temporal order. From scoreboard signals (Section 3), we derive a coarse hit label for each side (no hit, off-target, on-target) and prepend this information to the script.

The paired left/right scripts and hit labels are concatenated into a single *move sequence* string. We embed this string into a fixed-length dense vector using a sentence-transformer and perform semantic retrieval over a small rule database using FAISS [13]. The top- k most relevant snippets are retrieved and appended to the prompt used by the reasoning stage.

4.6. FERA-LM

FERA-LM applies rule reasoning to the combined move sequence and retrieved rule snippets. A fixed prompt defines the token format, summarizes a simplified subset of foil right-of-way rules (attack versus counterattack, parry-riposte chains, simultaneous actions), appends retrieved rules, and instructs the model to output a single priority decision (Left / Right / None) and a concise justification. We use DeepSeek-R1-Distill-Qwen-7B (off-the-shelf, no fine-tuning) as a demonstration that pose-derived multi-label tokens plus lightweight rule retrieval are sufficient for rule-grounded reasoning in foil exchanges [7].

5. Experiments

5.1. Setup and metrics

We evaluate move and blade recognition using 5-fold multilabel-stratified cross-validation on trimmed single-fencer segments. For each fold we construct training and held-out sets with similar label distributions and apply the data processing and augmentation pipeline described in Sections 3 and 4. Dynamic temporal windows and the 3-model ensemble are used only when deploying on continuous pose tracks, not for computing cross-validation metrics. Hyperparameters for FERA-MDT and the baselines are tuned on the first fold and then held fixed; all reported results use a single model per fold.

For move detection we report macro-, micro-, and weighted F1, Hamming loss, and calibration metrics (ECE,

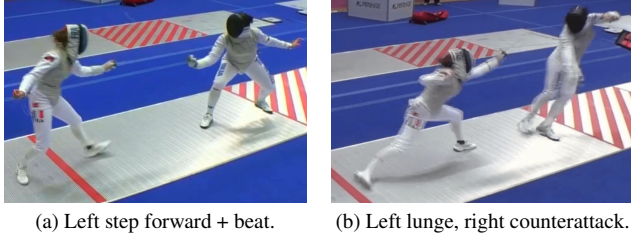


Figure 3. Frames from a bout where the referee awards priority to the left fencer.

MCE, and Brier score) [3, 8]. For the full pipeline, we report an end-to-end evaluation against referee priority decisions.

5.2. End-to-end performance

Figure 3 illustrates a bout where the referee awards priority to the left fencer. FERA-MDT predicts an attack sequence for the left (step forward into lunge + hit) versus retreat + counterattack for the right, and FERA-LM maps these tokens to a left-priority decision and a short explanation.

To quantify full-pipeline behavior, we compare FERA-LM decisions against referee priority rulings on an auxiliary set of 969 exchanges drawn from bouts disjoint from the cross-validation folds. We normalize the prefix label to obtain ground-truth priority and measure decision accuracy. FERA-LM matches the referee on 753 of 969 exchanges, yielding end-to-end accuracy of **77.7%**.

5.3. FERA-MDT and baseline details

BiLSTM baseline. A two-layer bidirectional LSTM (hidden size 128, dropout 0.2) followed by global average pooling and a linear head jointly predicts 12 move labels and 5 blade-line classes.

Temporal CNN baseline. A three-layer TCN (kernel size 3, 128 channels, dropout 0.2) with global average pooling and the same 17-way classifier head.

Blade-line prediction. Blade-line classification over positions (4, 6, 7, 8, other) uses the same backbone and a class-weighted cross-entropy loss. Across five folds we obtain macro-F1 of approximately 0.38: frequent blade lines (6 and 8) are recognized reliably, while rare positions (4, 7, other) remain the main source of error.

5.4. Co-occurrence analysis

Referee decisions depend on combinations of actions, so we assess whether models reproduce the ground-truth co-occurrence structure. For each fold, we form a move-move co-occurrence matrix by counting pairs of labels that are active in the same segment (ground truth) or predicted simultaneously (model). FERA-MDT most closely mirrors the ground-truth structure, while baselines tend to over-activate

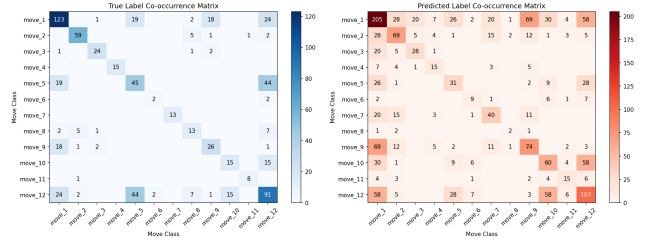


Figure 4. Co-occurrence mapping (Fold 5) for FERA-MDT. Left: ground truth. Right: predictions.

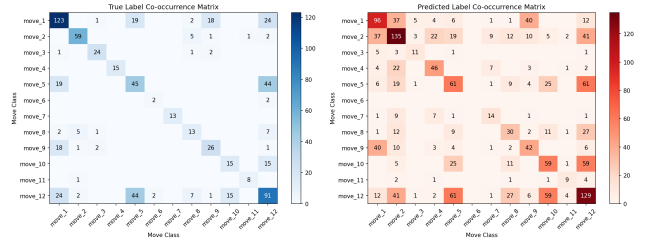


Figure 5. Co-occurrence mapping (Fold 5) for BiLSTM.

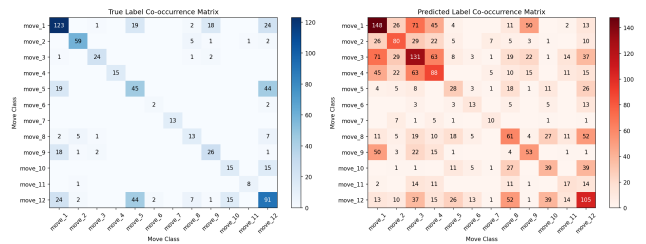


Figure 6. Co-occurrence mapping (Fold 5) for the TCN baseline.

frequent moves and underrepresent rarer co-occurring patterns.

5.5. Ablation study

To better understand which components drive performance, we ablate FERA-MDT while keeping the same folds, optimization schedule, and feature normalization. Each variant in Table 3 changes only one design choice (or one family of choices), so differences can be attributed to the corresponding component rather than to retraining noise.

Decision thresholds matter most for multi-label fencing.

Replacing tuned per-class thresholds with a fixed decision rule causes the largest drop in macro-F1 (0.549→0.511, -0.038). This is expected because the move distribution is highly imbalanced (Table 1) and classes differ substantially in base rate and separability: a universal threshold over-penalizes rare labels and under-penalizes frequent ones. In practice, per-class thresholding is therefore critical for deployment, where the cost of missing a rare but decisive action (e.g., parry/counterattack) can be higher than producing an occasional false positive on common footwork.

Table 2. Move detection performance compared with baselines. Values are mean \pm std over folds.

Model	Macro-F1 \uparrow	Micro-F1 \uparrow	Weighted-F1 \uparrow	Hamming \downarrow	ECE \downarrow	MCE \downarrow	Brier \downarrow
FERA-MDT (Ours)	0.549 \pm 0.018	0.539 \pm 0.021	0.549 \pm 0.009	0.162 \pm 0.016	0.107 \pm 0.019	0.390 \pm 0.045	0.137 \pm 0.007
BiLSTM [20]	0.537 \pm 0.014	0.537 \pm 0.014	0.558 \pm 0.011	0.166 \pm 0.010	0.080 \pm 0.009	0.461 \pm 0.063	0.136 \pm 0.002
TCN [2]	0.520 \pm 0.021	0.520 \pm 0.021	0.553 \pm 0.013	0.186 \pm 0.019	0.097 \pm 0.010	0.397 \pm 0.050	0.137 \pm 0.009

Engineered kinematics improve both recognition and reliability. Using only normalized joint coordinates (24D) reduces macro-F1 (0.534) and slightly worsens calibration metrics, confirming that scale-robust geometric features (distances, angles, torso orientation, arm extension) provide useful inductive bias for fencing-specific cues. Interestingly, removing temporal finite differences yields nearly unchanged macro-F1 (0.548) but substantially worse worst-case calibration (MCE 0.722), indicating that explicit motion cues help the model avoid highly overconfident errors even when they do not move the average F1.

Augmentation must respect temporal boundaries. Disabling augmentation moderately reduces macro-F1 (0.541), while using only temporal augmentation (e.g., time-warp/jitter) is harmful (0.525). This is consistent with our labeling protocol: segment boundaries are meaningful, and aggressive temporal perturbations can blur action onsets/offsets or distort short, sharp blade events. In contrast, noise-only augmentation preserves temporal structure and yields the best ECE (0.086), suggesting that small feature-space perturbations improve robustness without corrupting timing.

Calibration and loss balancing primarily affect downstream use. Temperature scaling and probability calibration have little effect on macro-F1 in our setting (“No calibration” matches 0.549) because F1 is dominated by decision thresholds, but calibration improves probability quality as reflected by lower MCE/Brier in the full model. Similarly, equalizing the move/blade loss weights slightly degrades performance (0.544), supporting our choice to balance gradient magnitudes so that the minority blade head is not under-trained.

Takeaway. Overall, the ablations suggest that (i) per-class thresholds are essential for good multi-label decisions under severe class imbalance, (ii) fencing-aware kinematics provide a measurable advantage beyond raw joints, and (iii) augmentation should emphasize mild, structure-preserving perturbations. These findings inform the practical configuration we use for end-to-end deployment and point toward future gains via better long-tail coverage and more explicit weapon cues.

6. Limitations and future work

Our study has several limitations that point toward promising directions for future work. First, data scale and imbal-

Table 3. Ablation study on FERA-MDT (5-fold cross-validation).

Variant	Macro-F1 \uparrow	ECE \downarrow	MCE \downarrow	Brier \downarrow
Full FERA-MDT (calibrated)	0.549	0.107	0.390	0.137
No augmentation	0.541	0.102	0.510	0.150
Raw joints only (24D)	0.534	0.103	0.480	0.149
Noise-only augmentation	0.542	0.086	0.411	0.141
Temporal augmentation only	0.525	0.120	0.552	0.164
No temporal features	0.548	0.093	0.722	0.140
No calibration	0.549	0.092	0.448	0.143
Equal move/blade loss weight	0.544	0.097	0.442	0.146
No per-class thresholds	0.511	0.090	0.346	0.138

ance remain significant. Manual frame-level labeling limits the number of segments, and rare actions (e.g., *flèche* and uncommon blade positions) are underrepresented. We expect further gains with additional data, particularly for long-tail actions.

Second, FERA currently relies on generic 2D pose estimates that do not capture the blade explicitly. Fencing-specific detectors or 3D pose could improve robustness to camera viewpoint and occlusion and provide more accurate information about blade orientation and contact.

Third, while FERA-LM performs reliably given valid inputs, we lack ground-truth textual explanations from referees for direct supervision. Our end-to-end accuracy is therefore a proof of concept; collecting structured referee justifications would allow a more thorough evaluation of explanation quality and help close residual gaps between model and human calls. Interestingly, despite moderate macro-F1 for moves and limited accuracy on rare blade positions, the system still recovers referee priority with 77.7% accuracy, suggesting that right-of-way decisions are robust to certain token-level errors.

Finally, we do not enforce athlete-disjoint splits because athlete identity is not consistently available. Our dataset spans roughly 130 competitors, but some overfitting to individuals remains possible. More reliable identity metadata would enable stronger generalization checks.

7. Conclusion

FERA demonstrates that pose-derived kinematics can support fine-grained, *multi-label* action recognition and downstream rule reasoning in real broadcast foil bouts. Starting from monocular 720p footage, our pipeline extracts per-fencer pose tracks, maps them into a canonical single-fencer representation via horizontal flipping, and encodes

each frame as a compact 101-dimensional descriptor that combines geometry (stance, arm extension, and torso orientation) with motion (first/second-order differences). A calibrated encoder-only transformer (FERA-MDT) then predicts co-occurring footwork and blade actions together with blade-line position, and a dynamic temporal windowing procedure enables deployment on untrimmed pose tracks without requiring explicit segment boundaries.

Across 1,734 clips with 2,386 annotated actions, FERA-MDT achieves a macro-F1 of 0.549 ± 0.018 under 5-fold cross-validation and outperforms BiLSTM and TCN baselines, while producing probabilistic outputs suitable for downstream decision support. Importantly, when paired with lightweight retrieval and a small language model (FERA-LM), these pose-derived tokens recover referee priority with 77.7% accuracy on 969 exchanges, suggesting that simplified right-of-way decisions are often robust to moderate token-level errors and that semantic grounding can be achieved without explicit blade reconstruction.

This work also highlights clear next steps. Performance is constrained by data scale and long-tail actions (e.g., flèche and rare blade positions), by the limitations of generic 2D pose estimation under occlusion and camera motion, and by the lack of ground-truth textual explanations for supervising explanation quality. Future work can pursue (i) additional labeling and targeted long-tail collection, (ii) fencing-specific perception—e.g., higher frame-rate footage, 3D pose, or explicit blade/tip cues when available, and (iii) tighter coupling between perception and reasoning, including calibrated uncertainty propagation, structured rule induction, and distillation of the reasoning stage for low-latency deployment. Overall, FERA provides a concrete case study of a reusable multimedia pattern—pose-level tokenization, calibrated temporal modeling, and lightweight rule reasoning—for decision support tasks where symbolic rules must be applied to fast human interactions.

References

- [1] Takuya Akiba, Shotaro Sano, Toshihiko Yanase, Takeru Ohta, and Masanori Koyama. Optuna: A next-generation hyperparameter optimization framework. In *Proceedings of the 25th ACM SIGKDD International Conference on Knowledge Discovery & Data Mining*, page 2623–2631, New York, NY, USA, 2019. Association for Computing Machinery.
- [2] Shaojie Bai, J. Zico Kolter, and Vladlen Koltun. An empirical evaluation of generic convolutional and recurrent networks for sequence modeling, 2018.
- [3] Glenn W. Brier. Verification of forecasts expressed in terms of probability. *Monthly Weather Review*, 78(1): 1–3, 1950.
- [4] Zhe Cao, Gines Hidalgo, Tomas Simon, Shih-En Wei, and Yaser Sheikh. Openpose: Realtime multi-person 2d pose estimation using part affinity fields. *IEEE Transactions on Pattern Analysis and Machine Intelligence*, 43(1):172–186, 2021.
- [5] Kai Chen, Jiaqi Wang, Jiangmiao Pang, Yuhang Cao, Yu Xiong, Xiaoxiao Li, Shuyang Sun, Wansen Feng, Ziwei Liu, Jiarui Xu, et al. Mmdetection: Open MMLab detection toolbox and benchmark. *arXiv preprint arXiv:1906.07155*, 2019.
- [6] Anthony Cioppa, Mehdi Chouiten, Pranav Chaudhari, Marco Ciaperoni, Mario Mezzani, Johannes T. Holz, Junqing Lv, Mitra Baratchi, Carlos H. M. De Souza, Hersh Shukla, Adriaan S. Hendricks, Silvio Giancola, Bernard Ghanem, Jan C. van Gemert, Cees G. M. Snoek, Hugo Mercier, Adrien Deliege, and Marc Van Droogenbroeck. Soccernet 2024 challenges results. In *Proceedings of the IEEE/CVF Conference on Computer Vision and Pattern Recognition (CVPR) Workshops*, pages 3256–3266, 2024.
- [7] DeepSeek-AI. Deepseek-r1-distill-qwen-14b (model card). <https://huggingface.co/deepseek-ai/DeepSeek-R1-Distill-Qwen-14B>, 2025. accessed: 2025-09-08.
- [8] Chuan Guo, Geoff Pleiss, Yu Sun, and Kilian Q. Weinberger. On calibration of modern neural networks. In *Proceedings of the 34th International Conference on Machine Learning*, pages 1321–1330. PMLR, 2017.
- [9] Jan Held, Anthony Cioppa, Hani Itani, Bernard Ghanem, and Marc Van Droogenbroeck. VARS: Video assistant referee system for automated soccer decision making from multiple views. In *Proceedings of the IEEE/CVF Conference on Computer Vision and Pattern Recognition (CVPR) Workshops*, pages 3179–3188, 2023.
- [10] Jan Held, Hani Itani, Anthony Cioppa, Silvio Giancola, Bernard Ghanem, and Marc Van Droogenbroeck. X-VARS: Introducing explainability in football refereeing with multi-modal large language model. In *Proceedings of the IEEE/CVF Conference on Computer Vision and Pattern Recognition (CVPR) Workshops*, pages 3267–3279, 2024.
- [11] Hugging Face. Distilgpt-2 (model card). <https://huggingface.co/distilbert/distilgpt2>, 2024. accessed: 2025-09-08.
- [12] Tao Jiang, Peng Lu, Li Zhang, Ningsheng Ma, Rui Han, Chengqi Lyu, Yining Li, and Kai Chen. Rtm-pose: Real-time multi-person pose estimation based on mmpose, 2023.
- [13] Jeff Johnson, Matthijs Douze, and Hervé Jégou. Billion-scale similarity search with gpus. *IEEE Transactions on Big Data*, 7(3):535–547, 2021.
- [14] Ilya Loshchilov and Frank Hutter. SGDR: Stochastic

- gradient descent with warm restarts. In *International Conference on Learning Representations*, 2017.
- [15] Ilya Loshchilov and Frank Hutter. Decoupled weight decay regularization. In *International Conference on Learning Representations*, 2019.
- [16] Chengqi Lyu, Wenwei Zhang, Haiyan Huang, Yue Zhou, Yudong Wang, Yanyi Liu, Shilong Zhang, and Kai Chen. Rtmddet: An empirical study of designing real-time object detectors, 2022.
- [17] Filip Malawski. Fencing footwork dataset (ffd). <https://home.agh.edu.pl/~fmal/ffd/>, 2016. accessed: 2025-09-08.
- [18] OpenMMLab. Mmpose: OpenMMLab pose estimation toolbox and benchmark. <https://github.com/open-mmlab/mmpose>, 2024. accessed: 2025-09-08.
- [19] Adam Paszke, Sam Gross, Francisco Massa, Adam Lerer, James Bradbury, Gregory Chanan, Trevor Killeen, Zeming Lin, Natalia Gimelshein, Luca Antiga, et al. PyTorch: An imperative style, high-performance deep learning library. In *Advances in Neural Information Processing Systems (NeurIPS)*, 2019.
- [20] M. Schuster and K.K. Paliwal. Bidirectional recurrent neural networks. *IEEE Transactions on Signal Processing*, 45(11):2673–2681, 1997.
- [21] TryoLabs. Norfair documentation. <https://tryolabs.github.io/norfair/2.2/reference/>, 2023. accessed: 2025-09-08.
- [22] TryoLabs. Norfair: Lightweight python library for real-time multi-object tracking. <https://github.com/tryolabs/norfair>, 2023. accessed: 2025-09-08.
- [23] Nicolai Wojke, Alex Bewley, and Dietrich Paulus. Simple online and realtime tracking with a deep association metric. In *2017 IEEE International Conference on Image Processing (ICIP)*, pages 3645–3649, 2017.
- [24] Thomas Wolf, Lysandre Debut, Victor Sanh, Julien Chaumond, Clément Delangue, Anthony Moi, Pierric Cistac, Tim Rault, Rémi Louf, Morgan Funtowicz, et al. Transformers: State-of-the-art natural language processing. In *Proceedings of the 2020 Conference on Empirical Methods in Natural Language Processing: System Demonstrations (EMNLP Demos)*, pages 38–45, 2020.
- [25] Bin Xiao, Haiping Wu, and Yichen Wei. Simple baselines for human pose estimation and tracking. In *Proceedings of the European Conference on Computer Vision (ECCV)*, pages 466–481, 2018.
- [26] Yufei Xu, Jing Zhang, Qiming Zhang, and Dacheng Tao. Vitpose: Simple vision transformer baselines for human pose estimation, 2022.
- [27] Yifu Zhang, Peng Sun, Yi Jiang, Dongdong Yu, Xinze Weng, Zhaoqi Yuan, Ping Luo, Wen Liu, and Xiaogang Wang. ByteTrack: Multi-object tracking by associating every detection box. In *Proceedings of the European Conference on Computer Vision (ECCV)*, 2022.
- [28] Kevin Zhu, Alexander Wong, and John McPhee. Fencenet: Fine-grained footwork recognition in fencing. In *CVPR Workshops*, 2022.